



# Tribological Tests Effect on Changes in the Surface Layers of Iron-Containing Antifrictional Aluminum Alloys

Aleksey M. Mezrin<sup>1\*</sup>, Olga O. Shcherbakova<sup>1</sup>, Tamara I. Muravyeva<sup>1</sup>, Dmitry L. Zagorskiy<sup>1,2</sup> and Ivan V. Shkalei<sup>1</sup>

<sup>1</sup> Laboratory of Tribology, Institute for Problems in Mechanics of RAS, Moscow, Russia, <sup>2</sup> Physics Chair Department, I.M.Gubkin Oil and Gas University, Moscow, Russia

## OPEN ACCESS

### Edited by:

Alessandro Ruggiero,  
University of Salerno, Italy

### Reviewed by:

Jose Daniel Biasoli De Mello,  
Federal University of Uberlandia, Brazil

Roberto D'Amato,  
Universidad Politécnica de Madrid  
(UPM), Spain

### \*Correspondence:

Aleksey M. Mezrin  
ammezrin@gmail.com

### Specialty section:

This article was submitted to  
Tribology,  
a section of the journal  
Frontiers in Mechanical Engineering

**Received:** 17 January 2019

**Accepted:** 21 March 2019

**Published:** 10 April 2019

### Citation:

Mezrin AM, Shcherbakova OO,  
Muravyeva TI, Zagorskiy DL and  
Shkalei IV (2019) Tribological Tests  
Effect on Changes in the Surface  
Layers of Iron-Containing Antifrictional  
Aluminum Alloys.  
Front. Mech. Eng. 5:14.  
doi: 10.3389/fmech.2019.00014

Antifrictional properties and surface parameters of Al-Si-Cu-Sn-Pb alloys have been investigated. The effect of iron addition (~1%) on the structure and tribological properties of aluminum alloy samples has been studied. Tribological properties were explored using the “shoe-roller” scheme with step-by-step pressure changes. The investigations were carried out both in and without a lubricant. The SEM- (with elemental analysis) and SPM-microscopy methods were applied to study sample surface and under-surface layers of the samples at the transversal sections. After tribological tests have been carried out, the topography of both surface and under-surface layers at the transversal sections has been studied. During the tests without lubrication solid particles, presumably, oxides were formed. The particles increase the surface destruction, thus, doing their part of an abrasive and contributing to (scuffing) score. After testing in the lubricant particles containing silicon and copper and having a rounded shape were also formed. These particles remain on the surface and are rolled in the lubricant. They creating a kind of a “protective cover” contributing to the contact pair stable operation. The under-surface layer 50–100 μm thick formation was found at the sections after tribological tests without lubrication. The samples sections were prepared after testing with lubrication. The study of the samples sections demonstrated the formation of the under-surface layer with thickness 30–40 μm. The elements redistribution in these layers was shown. After the tribological tests were carried out, the counterbodies (rollers) were also explored. The SPM method has been shown the film formed on the surface is uneven in thickness after tests without lubrication. This leads to the macrorelief development during friction and can lead to (scuffing) score. On the contrary, after tests in lubricant the secondary structures film formed is distributed on the surface as a thin uniform layer. This film has the protective properties. It was shown that alloys containing iron (up to 1%) have good tribological characteristics when tested both in and without the lubricant. Thus, they can be used as antifrictional materials.

**Keywords:** antifrictional alloys, tribological tests, wear resistance, surface and under-surface layers, microscopy

## INTRODUCTION

In engineering, an important task is to increase the tribological properties of materials used in friction units, in particular, in plain bearings. Different types of antifriction materials could be used for construction of mechanical units. Most often, alloys based on expensive copper (bronze) are used in bearing assemblies. Recently, aluminum alloys doped with low-melting metals have also been used. The replacement of bronze by aluminum alloys is due to a good combination of their technological and tribological properties at a relatively low cost. The authors of Mironov et al. (2015) compared standard antifriction bronzes and new antifriction aluminum alloys. The results of their research showed that experimental aluminum alloys have high tribological properties, in particular, increased score-resistance (compared to bronze) in combination with high strength. It was shown in Mironov et al. (2017) that the mechanical and tribological properties of aluminum alloys can be changed by changing the content and concentrations of various alloying elements. The main result of doping is the presence of low-melting elements (soft phase component). These elements extract out to the surface and play the role of a solid lubricant under critical conditions.

A large amount of theoretical and experimental work is devoted to the study of friction processes and the change of contact surfaces. In these works, the features of these alloys are considered—the extraction of a soft phase from a solid matrix, mass transfer from one friction surface to another, the formation of a film of secondary structures (SS). In Bushe et al. (2003), the authors presented an improved model of the process of separating the soft phase from the antifriction alloy. This model takes into account the fact that the amount of plastic phase that forms the SS film depends on the nature and strain value of the matrix itself. A model applicable to a two-phase material, where the phase inclusions are in a state of plastic flow, which is typical for antifriction alloys, is presented in Bravo et al. (2013). It was assumed that the entire volume is more pliable, compared to the matrix, the phases from the surface layer is transferred to the surface of the material, creating a protective film of the SS. In Zhang et al. (2016) changes on the surface and in the near-surface region of the antifriction material were investigated. The process of low-melting phase behavior during friction was shown and its effect on the friction coefficient and wear rate was estimated. In Gershman and Bushe (2004), it was shown that during contact interaction, a protective film of SS is formed on the surface of a steel shaft, which is created by transferring a soft phase (low-melting elements) from a hard alloy bearing shell. In the process of mass transfer, a change in the topography and elemental composition of the contact surfaces occurs. In Stolyarova et al. (2017) it is shown that destruction is a multi-step process. The stages of this process are not only the transfer of material from one friction surface to another, and the change in the surface topography, but also the score. All these processes occur differently in different conditions and for different materials.

Another important task is to improve and modify the properties of the alloys, achieved by improving their

composition and selection of optimal heat treatment conditions. Thus, the authors of Belov et al. (2016b) showed that the Al-Si-Cu-Sn-Pb alloys have a good combination of properties, and the optimal mode of their heat treatment is annealing at 500°C with cooling in water and subsequent aging.

A very promising idea is the use of aluminum alloys with iron impurities. Interest in such materials is due to the potential possibility of making alloys from cheaper materials and their own production waste. This would reduce the cost of the products. However, the inevitable consequence of this will be the appearance of iron in the composition of the final product. It is known that iron is often a harmful impurity, leading to the degradation of the plastic properties of a material (Belov et al., 2002). To neutralize this effect, manganese is added to aluminum alloys. Alloys of similar compositions were studied by the authors in previous works (Sachek et al., 2018), in which it was shown that the addition of iron (up to 1%, together with manganese) does not lead to a noticeable degradation of the tribological properties of the alloys.

The aims of this work were to study samples of iron-containing experimental aluminum alloys—their tribological properties, structure and elemental composition of the surface and surface layers. The study of changes in these properties was carried out in two modes of tribological tests—in lubrication and without it. The main goal of this work was to estimate the possibility of using iron-containing aluminum alloys as anti-friction materials.

## MATERIALS AND METHODS

### Materials

The compositions of the investigated aluminum alloys are given in **Table 1**. The main object of study was aluminum alloy Al-5% Si-4% Cu-6% Sn with the addition of iron (about 1%, alloy 1) and other elements. To neutralize the harmful effects of iron, small amount of manganese (0.5%) was added to this alloy. The properties of this alloy were compared with the properties of three others aluminum alloys of similar composition, but without the addition of iron (alloys 2–4). These alloys were selected from a series of aluminum alloys, obtained on the basis of phase diagrams presented in Belov et al. (2016a,b). The selection criteria were the results of sclerometric tests (Sachek et al., 2016), which showed that these alloys have the best tribological properties. Alloy No. 3, which does not contain low-melting metals, was taken as the base composition. Alloy No. 4 contains a small amount of low-melting alloying elements (about 1% Bi), and in alloy No. 2 it contains 6% (5% Sn and 1% Pb). All low-melting elements (Sn, Pb, and Bi) were added to the iron-containing alloy No. 1, but their total amount practically corresponded to alloy No. 2.

After fabrication, the cast alloys were heat treated—annealed at 500°C, followed by quenching in water and aging. This treatment was selected based on previously obtained results (Belov et al., 2016b).

**TABLE 1** | The chemical composition of the investigated alloys.

| Sample | Chemical composition (% mass.) |     |     |       |     |       |     |     |            |
|--------|--------------------------------|-----|-----|-------|-----|-------|-----|-----|------------|
|        | Al                             | Si  | Cu  | Sn    | Pb  | Bi    | Fe  | Mn  | Impurities |
| No 1   | 82,80                          | 5.1 | 4.3 | 5.6   | 0.4 | 0.4   | 0.7 | 0.5 | <0.2       |
| No 2   | 84,30                          | 4.9 | 4.2 | 5.5   | 1.0 | <0.01 | –   | –   | <0.1       |
| No 3   | 91,10                          | 4.8 | 3.9 | –     | –   | –     | –   | –   | <0.2       |
| No 4   | 89,30                          | 4.6 | 4.1 | <0.01 | 0.7 | 1.2   | –   | –   | <0.1       |

## Sample Preparation

The surface of the alloy before and after testing was investigated in this work. To study the initial surface, thin sections were prepared using the “TegraPol-25” and “TegraForce-5” complex (Struers). To study the surface layer after testing, an Accutom-5 programmable cutting machine (Struers) was used to make a transversal section of the alloy sample (at the 45° angle), which was then grounded and polished. The above works were carried out according to standard methods.

## Tribological Tests

Tribological tests were carried out on the T-05 tribometer according to the “block-on-ring” (ASTM G77) scheme. Material of the ring (counterbody, roller) is Steel 45 and materials of the block (shoe) are experimental alloys under study. This contact pair was studied according to the previously developed method (Sachek et al., 2015). For testing with lubrication, the counterbody was partially immersed in the lubricating medium so during rotation the lubricant was captured by the counterbody and drawn into the contact zone. Alloy samples were tested both in lubrication (motor oil for diesel engines 5W-40 was used) and without it (dry).

In both cases, the studies were performed with stepwise changes of the pressure until reaching a scuffing. The minimal pressure for tests without lubrication was 0.2 MPa and for tests with lubrication it was 3.2 MPa. The number of repetitions for each value of pressure was 2–3.

## Surface Microscopy

Scanning electron microscopy was the main method for investigation of the surface. The SEM “FEI QUANTA 650” with an EDAX elemental analysis tool was used. The image was obtained using two detectors, the secondary and the back-scattered electrons. Accelerating voltage of 25 kV was used. The measurements were carried out in vacuum; no special surface preparation was required. SEM surface studies were performed before and after tribological tests.

Scanning probe microscopy was used to study the surface at the micro- and nano-levels: SPM SmartSPM TM (AIST-NT) was used. Taping mode was applied (AIST-NT cantilevers, fpN10, cantilever stiffness –10–20 N/m, resonant frequency 200–300 kHz). Scanning field was 100 × 100 μm. SPM studies were carried out on the original surface.

## RESULTS AND DISCUSSION

### Examination of the Samples Structure

To study the initial surface of the experimental alloy, both in the cast and in the heat-treated state, a complex microscopic examination technique was used (Belov et al., 2016b). This technique involves applying special markers (benchmarks or “reference marks”) on the surface. This makes it possible to select and examine the same surface areas when using different methods of microscopy (electron and probe microscopies).

**Figure 1**<sup>1</sup> shows the obtained SEM and SPM images of polished surfaces of the original samples—both cast and after heat treatment.

The method of “reference marks” allowed to correlate the SEM and AFM data and identify individual phases. X-ray analysis (in the SEM) made it possible to determine the elemental composition of the individual phases, while their spatial geometry was investigated using the AFM method. It should be noted that the use of AFM made it possible to identify the phases that couldn’t be detected at the SEM image (Thus, the silicon phase in the aluminum matrix is very poorly visible due to the proximity of atomic numbers).

As was shown earlier (Belov et al., 2016b; Stolyarova et al., 2017), heat treatment changes the structure of the alloy. In this work, a comprehensive analysis of the polished surface confirmed that after heat treatment, the silicon and soft phases acquired a rounded shape, the copper content decreased (due to its partial dissolution in the aluminum matrix). The experimental alloy also revealed an iron-containing phase [Al<sub>15</sub>(Fe, Mn)<sub>3</sub>Si<sub>2</sub>], which has a specific “skeletal” form (see **Figure 1**). It is known that usually in an aluminum alloy with iron a “needle-like” phase is formed, which causes embrittlement of the alloy. In this case, the addition of manganese neutralizes the harmful effects of iron and promotes the formation of the phase of the “skeleton” form, which does not impair the properties of the alloy (Sachek et al., 2018). It was also revealed that heat treatment does not affect this phase.

### Tribological Tests

To study the effect of iron addition to the composition of aluminum alloys on its tribological characteristics, comparative wear tests of alloys with iron (No. 1) and without it (No. 2, 3, 4) were carried out according to the “block-on-ring” scheme. The tests were carried out at a constant sliding speed with a stepwise increasing load for two cases: without lubrication and with lubrication. The mode without lubrication (express tests) was used to reduce the duration of the tests. It also gave the opportunity to study the behavior of the alloy in the extreme mode of operation (it is known that these materials belong to so-called “self-lubricating” materials). Working in lubrication is a normal mode of operation of such materials in friction units.

The dependences of the wear intensity on the contact pressure were obtained by processing of the experimental data. The results

<sup>1</sup>Hereinafter, modified images are given. This is done to improve their perception and interpretate displayed information. Original images received by the devices are given in **Supplementary Material**.

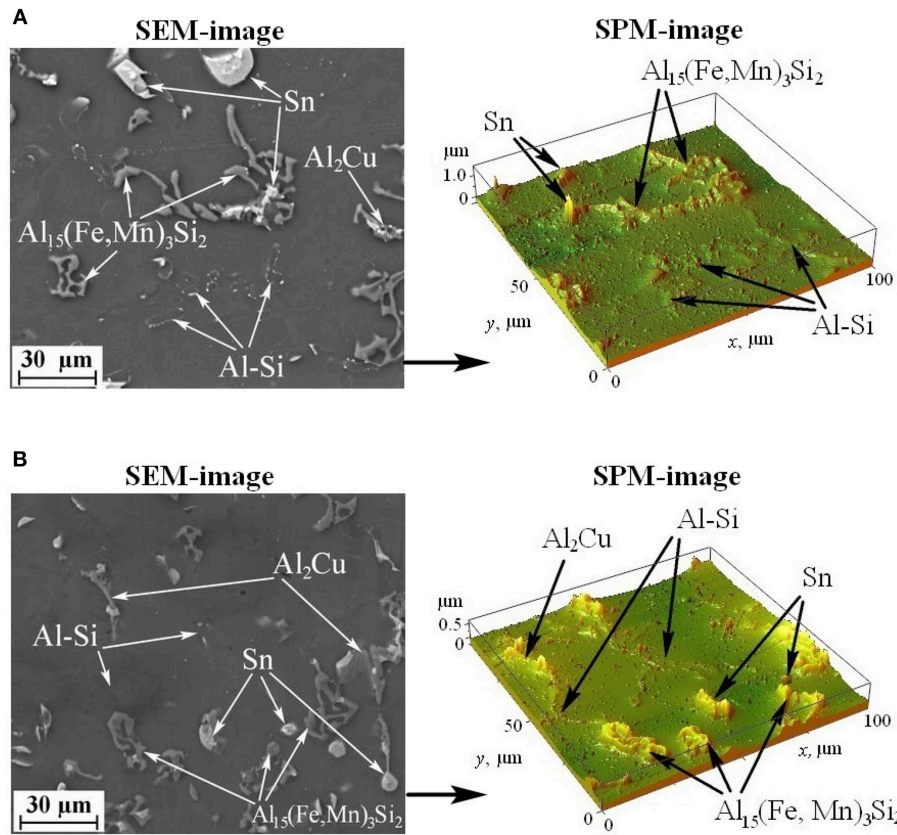


**FIGURE 1** | SEM and SPM (3D) images of the polished surface of the experimental alloy No. 1: **(A)** in the cast state, **(B)** in heat-treated state.

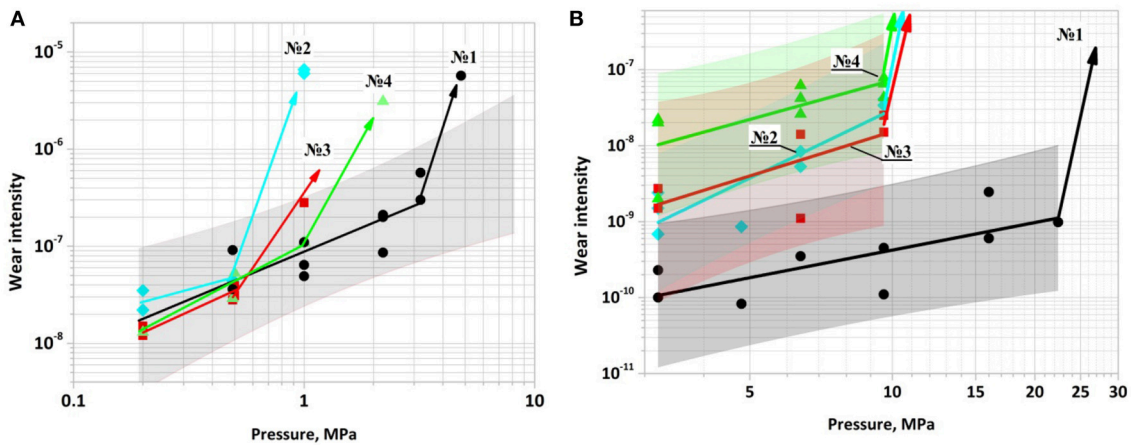


**FIGURE 2** | The dependence of the wear intensity (data points, approximation lines and 95% confidence bands) of the investigated alloys on the contact pressure in two modes: **(A)** without lubricant, **(B)** with lubricant. (No. 1–No. 4 are numbers of alloys).

for two cases, without lubrication and with lubrication, are presented in the graphs (Figure 2).

A critical pressure at which the scuffing was observed for each alloy is presented in the Table 2. In some cases at a pressure above critical, due to the rapid destruction of the sample, it was

not possible to estimate its wear intensity. Linear regression was done for pressure range up to critical level. The beginning of scuffing is indicated by arrows on the graphs. At pressures up to a critical level 95% confidence bands and the wear equation for all alloys, were tested without lubrication, appeared approximately

**TABLE 2** | Critical pressure and wear equation when tested for wear of the studied alloys without lubrication and with lubrication.

| Sample | Without lubrication    |                                 |                       | With lubrication       |                                    |                      |
|--------|------------------------|---------------------------------|-----------------------|------------------------|------------------------------------|----------------------|
|        | Critical pressure, MPa | Wear equation                   | Mean square error     | Critical pressure, MPa | Wear equation                      | Mean square error    |
| No 1   | 2–3                    |                                 |                       | 23                     | $I_1 = 2.6 \cdot 10^{-11} p^{1.2}$ | $3.2 \cdot 10^{-10}$ |
| No 2   | 0.5                    | $I = 1.8 \cdot 10^{-8} p^{0.7}$ | $< 7.0 \cdot 10^{-8}$ | 10                     | $I_2 = 3.1 \cdot 10^{-11} p^{3.0}$ | $3.7 \cdot 10^{-9}$  |
| No 3   | 0.5                    |                                 |                       | 10                     | $I_3 = 1.8 \cdot 10^{-10} p^{1.9}$ | $5.0 \cdot 10^{-9}$  |
| No 4   | 1                      |                                 |                       | 10                     | $I_4 = 1.4 \cdot 10^{-9} p^{1.7}$  | $2.0 \cdot 10^{-8}$  |

the same. On the left graph confidence bands are shown in gray only for alloy No. 1.

According to critical pressure, alloy No. 1 with the iron content turned out to be the best. This alloy during the unlubricated friction test withstood a contact pressure of 2–3 MPa. The mean square error for all alloys is not  $> 7.0 \cdot 10^{-8}$ .

It has been shown that during tests with lubrication, the process of wear of alloys proceeds more evenly, but at a pressure above the critical, a score also take place. It is seen that for iron-containing alloy (No. 1) the critical pressure is two times higher than for other alloys. In addition, this alloy showed the wear rate by 1–2 orders of magnitude lower than the other alloys and less dependence on pressure. For example, at pressure  $P = 10$  MPa the wear intensity of alloy No. 1 is  $I_1 = 4 \cdot 10^{-10}$  and for other alloys (No. 2–4) is  $I = (1.4 \dots 7) \cdot 10^{-8}$  (35–175 times higher). The dependence on pressure is indicated by the magnitude of the degree at P in the wear equation (Table 2).

According to the obtained results, it can be concluded that alloy No. 1 (containing iron) exceeded in all tribological parameters alloys No. 2, 3, 4 both in normal operation (i.e., in a lubricating medium) and in extreme operation (in the mode of lack of lubrication).

## The Study of the Surface of the Contact Pair After Tribological Tests Without Lubrication

After carrying out tribological tests without lubrication, changes in the contact zone were studied. Figure 3 shows the SEM images of the surface of the contact pair (pads of experimental alloy and steel roller) after testing at the pressure of 2.0 MPa.

As can be seen from Figure 3, a noticeable change in topography and composition took place on the surfaces of the shoe and roller. It is known that a change in conditions in the contact zone (in particular, an increase in pressure and temperature) can cause elastoplastic deformations of the surface and near-surface layers of rubbing bodies (Rigney, 2000). At the same time, on the contact surfaces, a complex of mechanical and physicochemical processes takes place, during which the material of shoe is transferred to the steel surface of the roller, contributing to the formation of a film of secondary structures. In extreme conditions of friction unit operation, a further increase of pressure and temperature in the contact zone leads to plastic flow of the shoe material and more intensive mass transfer. These processes lead to the formation of stuck and the development of relief on the roller (Figure 3B).

The SEM images of the surface of the roller presented on Figure 3B. It is possible to see the longitudinal strips and areas, which are different from the material of the roller in color and chemical composition. Thus, it was found that friction between two homogeneous materials occurs in the contact zone (“aluminum transferred to the roller—aluminum of the block”). Adhesion of homogeneous materials is higher—therefore, the development of macrorelief on the roller occurs. This leads to deformation and partial destruction of the shoe material (the formation of longitudinal grooves and caverns is shown on the surface—Figure 3A).

However, it is difficult to determine the film thickness (the most important parameter) from the SEM images. To estimate this thickness on the roller, an SPM method was used. The studies were done on the maximal scanning area for a given microscope— $100 \times 100 \mu\text{m}$ . The areas on the border of the “steel surface of the roller—film of secondary structures” were selected.

The results are presented in Figure 4 where SPM—image of the roller surface areas is shown. It can be seen that the roller is only partially covered with film, and the film itself has a developed structure. To determine the film thickness, section lines were made. The profile of such line is shown in Figure 4.

Several different areas were studied on the surface of the roller, which showed that the layer is unevenly distributed on the surface and varies significantly in thickness. In average, the thickness varies in the range of 1–2  $\mu\text{m}$ .

## Tests With Lubricant

After tribological tests with lubrication, studies of the shoe and roller surfaces were carried out. The obtained SEM images of the surfaces of the contact pair (tested at the pressure of 20 MPa) are presented in Figure 5.

Studies have shown that significant changes have occurred on the surfaces of the contact pair tested in lubrication. It is easy to see the formation of strips, the direction of which obviously coincides with the direction of friction: these strips are more pronounced on the surface of the roller than on the surface of the shoe. On the surface of the shoe you can see a lot of particles of rounded shape. Perhaps their form is associated with “running around” during the process of friction in a liquid oil medium. Of interest is the presence of elements and their distribution over the surface.

Comparison of SEM images and mapping results showed that the detected round-shaped particles contain a lot of silicon and copper (in the form of the eutectic Al-Si compound and the  $\text{Al}_2\text{Cu}$  compound, respectively). Obviously, these particles have

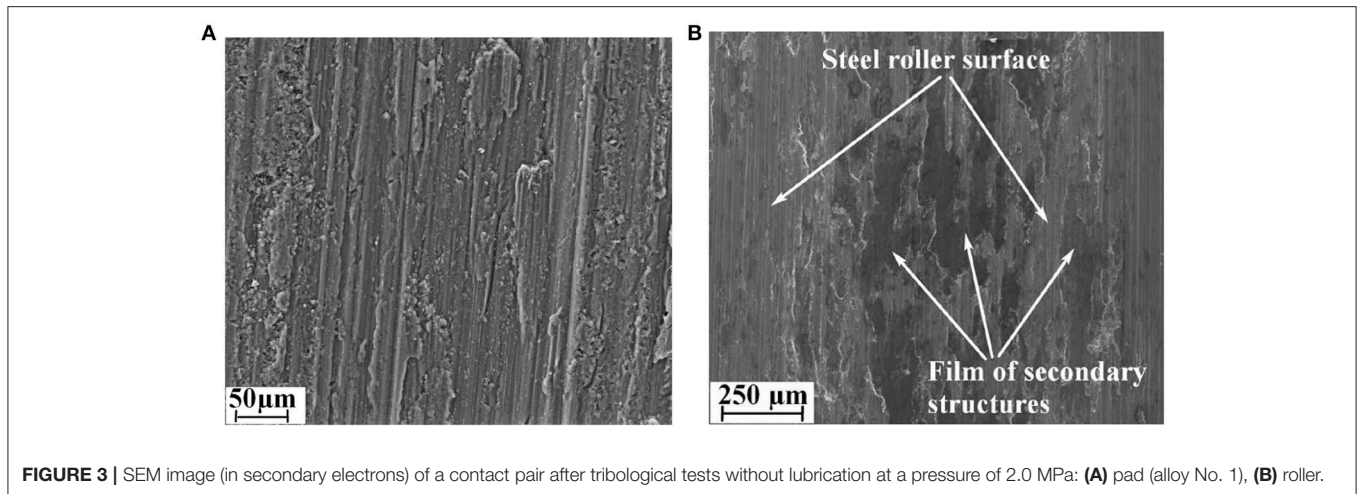


FIGURE 3 | SEM image (in secondary electrons) of a contact pair after tribological tests without lubrication at a pressure of 2.0 MPa: (A) pad (alloy No. 1), (B) roller.

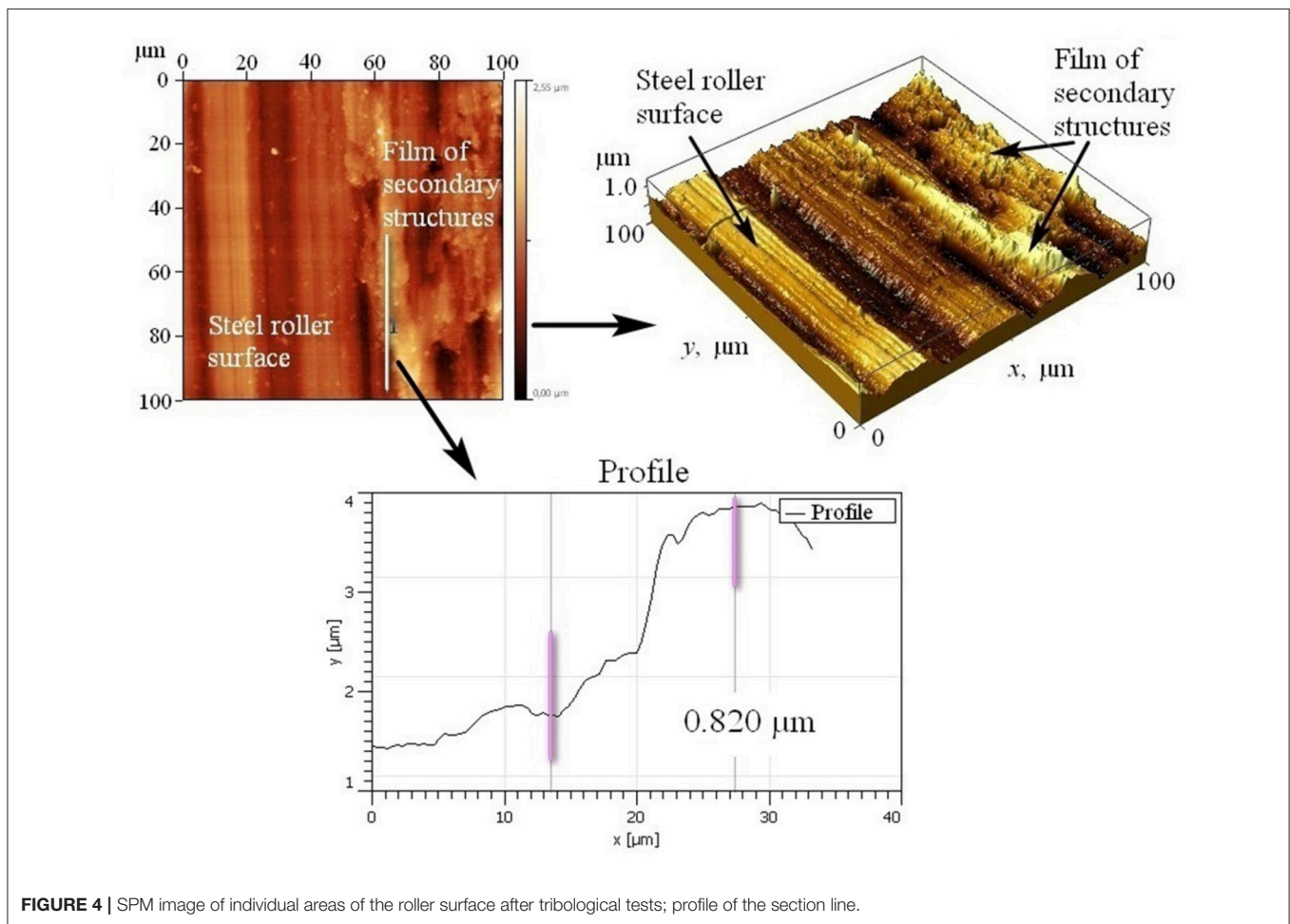
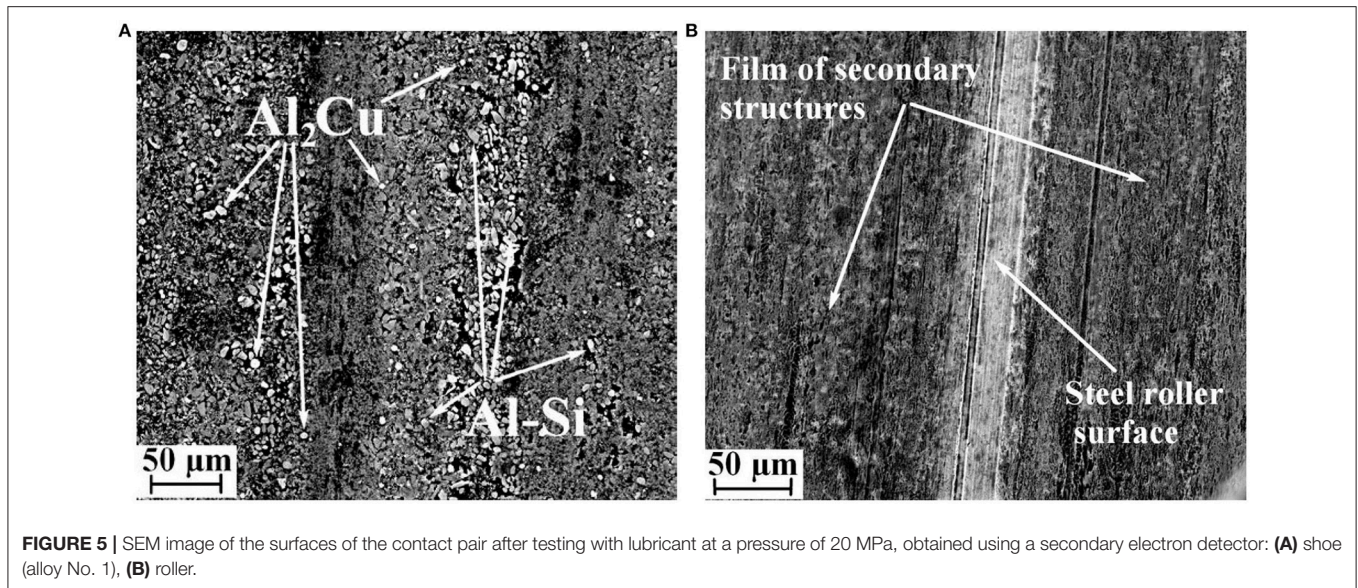


FIGURE 4 | SPM image of individual areas of the roller surface after tribological tests; profile of the section line.

a high hardness. On the surface of the roller (Figure 5B), a film of secondary structures (SS) was found, the formation of which is due to the process of mass transfer of chemical elements from the surface of the shoe in the contact zone.

The results of the SPM study of the roller after testing in the lubricant are presented in Figure 6.

The results obtained confirm and complement the data of electron microscopic studies. In Figure 6, a new phase is clearly visible, which appeared on the surface of the roller after the tests, which is the film of secondary structures. To estimate its thickness, a secant 1 (Figure 6) was carried out at the boundary of two



phases. The results of measurements are also presented in **Figure 6**.

SPM studies of the surface of the roller after tribological tests in lubricant showed that the film of secondary structures is evenly thin layer distributed on the surface and has a thickness of about 0.1  $\mu\text{m}$  (thickness is an order of magnitude less than when tested without lubrication). In this case, the film of secondary structures protects the surface of the roller from wear.

Thus, in both cases (test without lubrication and with lubrication) the film of secondary structures was formed. But this film, formed during the tests without lubrication, is unevenly distributed on the surface and has a developed relief (unlike film, formed during the tests with lubricant). Further development of this relief (with increasing pressure) can lead to a score.

### The Study of the Under-Surface Area of the Alloy (on the Transversal Sections) After Tribological Test

The structure of the material of the under-surface layer, and consequently its properties change during friction. This is due to plastic deformation in the contact zone, when mechanical energy is transferred to thermal energy (Schouwenaars et al., 2007). Oblique sections (slice cuts, transversal sections) of the shoe were prepared after the tests for a detailed study of the processes occurring during friction. These sections made it possible to study the changes occurring in the surface layers of the material, both in the friction mode without lubrication and with lubrication.

#### Tests Without Lubrication

The image of the slice of the shoe of the studied alloy and the mapping of the main elements after tribological tests without lubrication are presented in **Figure 7**.

It can be seen that changes occurred in the surface layer 50–100  $\mu\text{m}$  thick. Studies of the transversal sections of the

shoe (**Figure 7**) showed that in the under-surface layers, the soft phases were homogeneously redistributed (mixed) (**Figure 7**). Obviously, this is due to a significant increase in temperature in the contact zone. At the same time, the refractory (high-melting) phases (the eutectic compound Al-Si and  $\text{Al}_2\text{Cu}$ ) remained in the near-surface layers without changing their configuration (**Figure 7**). X-rays elemental analysis demonstrated that the quantity of Fe-contained phase in near-surface areas changed insignificantly to compare with the bulk. Therefore, the homogeneous distribution of Fe could be concluded.

In addition, the formation of cracks is evident; obviously, its occurrence is associated with extreme operating conditions. The development of such cracks leads to scaly exfoliation of the material and the subsequent destruction of the sample. It is known that under extreme conditions (without lubrication) a large friction force leads to an increase in the maximal tangential stresses of the sample and, as a result, to the formation of periodic microcracks on its surface. These microcracks extending inward in the direction of maximum tangential stresses (Panin et al., 2010). Under the influence of friction, these cracks open, forming a scaly surface structure, followed by the separation of wear particles that have a flat shape. However, due to the inhomogeneous structure of the alloy with the presence of solid particles, the development of some cracks is stopped. As example **Figure 7** shows an enlarged fragment of the longitudinal section of the tested shoe. It can be seen that the crack propagation ends on a solid inclusion ( $\text{Al}_2\text{Cu}$ ). Thus, the structure of the alloy prevents the development of cracks in the process of friction in the extreme mode, thereby ensuring greater wear resistance and load capacity, which is confirmed by the results of tribological tests (see **Figure 2A**).

#### Tests With Lubricant

Under-surface layers were also studied for samples after tests in lubrication. For this, the transversal section

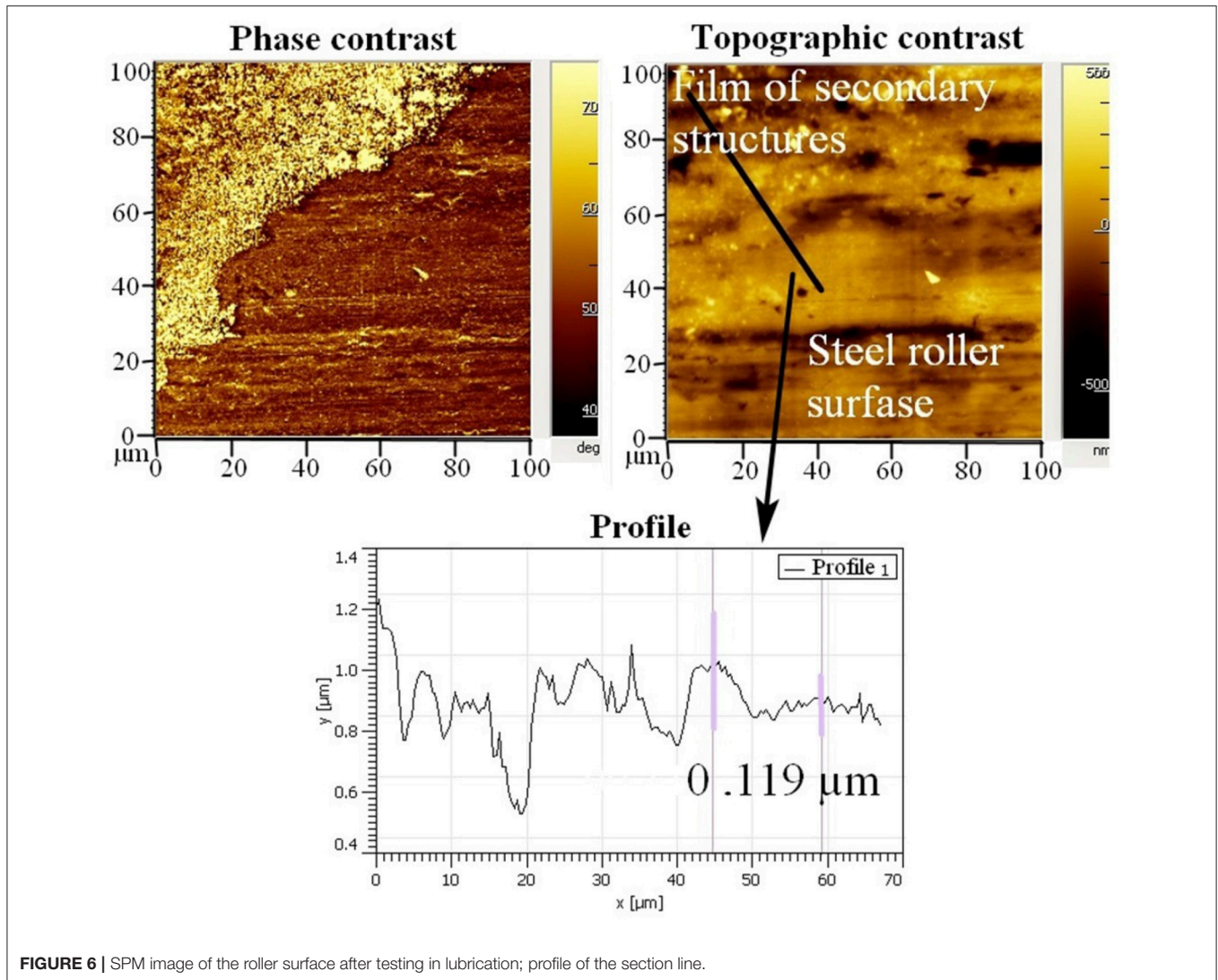


**FIGURE 6** | SPM image of the roller surface after testing in lubrication; profile of the section line.

of shoe was prepared. Resulting SEM image is shown in **Figure 8**.

On the obtained images one can clearly distinguish the near-surface layer, whose thickness is 30–40  $\mu\text{m}$  (Note that in section Tests Without Lubrication “Tests without lubrication,” where the tests were carried out in the dry friction mode at pressures an order of magnitude less, the thickness of the modified layer was about 2–3 times more obviously, this difference is determined by the difference in friction modes). It is seen that the structure of this layer differs markedly from the structure in volume. For example, some phase components, ordered in the direction of friction (“tracks”) are found. X-ray spectral analysis and mapping were performed to determine the elemental composition on the transversal section. The mapping results for the main alloying components are presented in **Figure 8**.

Using the above data, it is possible to determine the composition of the “tracks,” which are tin phases. Obviously, tin comes to the surface from the volume in the process of friction.

This is due to the fact that the grains and dendritic cells of the aluminum matrix are deformed in the surface layer in the process of friction. This leads to the extrusion of a low-melting tin phase onto the surface of the shoe. With increasing pressure on the rough contact surfaces, microstitching (microseizure) occurs, leading to a mass transfer process (tin, together with other elements, is transferred to the counterbody). This process leads to the formation of a protective film of secondary structures. Also, it is possible to determine the distribution of the refractory and iron-containing phases on the transversal section of the shoe. During the process of friction such phases are concentrated on the surface in the form of rounded particles. These particles create an additional frame that prevents further destruction of the soft aluminum matrix.

Note that in tests with lubricant, in contrast to tests without lubrication, a lower friction force creates lower shear stresses, which are insufficient to lose shear stability of the material—so, no cracks are formed in the material.



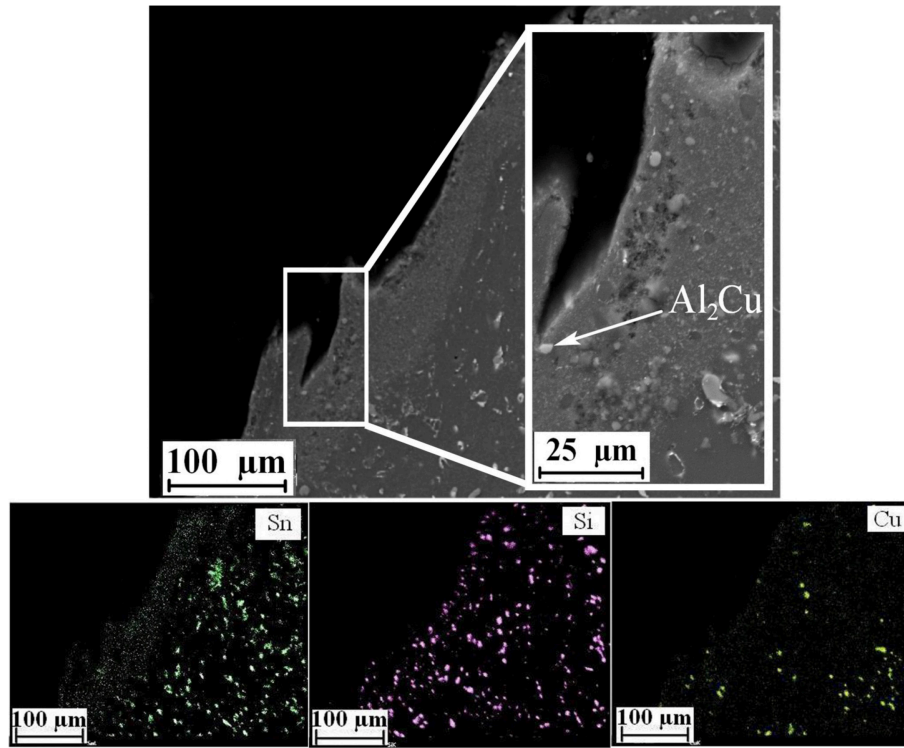


**FIGURE 7** | SEM image of the transversal section surface of the block of iron-containing alloy after tribological tests without lubrication; mapping for the main alloying elements.

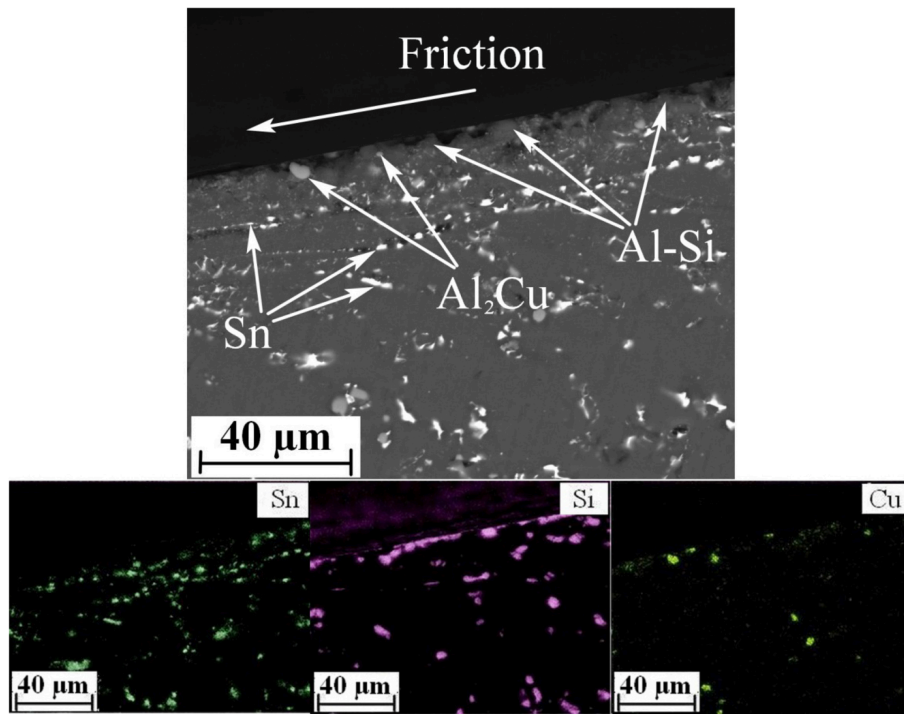


**FIGURE 8** | SEM image (in secondary electrons) of the surface of transversal section of the shoe (alloy No. 1) after tribological tests with lubrication. Corresponding mapping (the main alloying elements).

## CONCLUSIONS

Tribological tests in combination with various electron microscopic methods made it possible to study in detail the processes occurring on the surface and in the under-surface layer of the alloys during the friction tests.

- It is shown that the addition of iron to the composition of the alloy leads to an increase in wear resistance, both when tested in lubricant and without it;
- All the alloys under investigation (during tribo-testing) had a score at much higher pressures in the lubricated mode than in mode without lubrication. At the same time, for an iron-containing alloy, the critical pressure (after which the score occurs) is significantly higher than that for other alloys. This is explained by the fact that the iron-containing phases are solid inclusions and together with the phases  $Al_2Cu$  and Al-Si create an additional framework, preventing further destruction of the soft aluminum matrix. It is shown that the wear rate of this alloy is 1–2 orders of magnitude lower than that of other studied alloys. In addition, this parameter in the iron-containing alloy has a lower dependence on pressure;
- For all alloys during tribological tests in the unlubricated mode, the score occurs when the pressure increase. However, for the iron-containing alloy, this occurs at higher pressures—about twice higher than for other alloys;
- A characteristic relief develops on the surface of contact pairs during tribological tests. In the subsurface layers of the alloys under investigation (shoe), after testing in lubrication, a change in the arrangement of the elements is observed—first of all, the extrusion of tin to the surface. Mass transfer, contributing to the formation of the film of secondary structures, take place in the process of friction (due to mechanical and physicochemical processes occurring on the surface of the contact pairs). Film of this structures on the surface of the roller may play a different role depending on the conditions of experiment. So, in the case of friction

without lubrication (with the development of macrorelief), it can contribute to the formation of a score. At the same time, it plays a protective role during friction with lubricant;

- It was found that the growth of cracks, which are one of the causes of the score, in some cases can stop, possibly due to the interaction with the inclusions of solid phases;

So, the rather high tribological properties of iron-containing aluminum alloys are identified and explained. The alloy can be used both in lubrication and in critical friction modes. Thus, the possibility and prospects of using recycled iron-containing raw materials (waste) in the production of antifriction aluminum materials is shown.

## AUTHOR CONTRIBUTIONS

AM: tribology tests, tribology data analysis, and interpretation; OS, TM, DZ, and IS: complex microscopically analysis.

## FUNDING

This work was financially supported by the Federal Agency of Scientific Organizations (Reg. No. AAAA-A17-117021310379-5) (tribological tests) and partially supported by Grant of President of RF (MK-871.2018.8 No-AAAA-A18-118080290023-0) (microscopy investigations).

## ACKNOWLEDGMENTS

The authors are thankful to Prof. N. A. Belov (National University of Science and Technology MISIS) for submitting of the samples.

## SUPPLEMENTARY MATERIAL

The Supplementary Material for this article can be found online at: <https://www.frontiersin.org/articles/10.3389/fmech.2019.00014/full#supplementary-material>

## REFERENCES

- Belov, N., Aksenov, A., and Eskin, D. (2002). *Iron in Aluminium Alloys*. London: CRC Press. doi: 10.1201/9781482265019
- Belov, N. A., Stolyarova, O. O., Murav'eva, T. I., and Zagorskii, D. L. (2016b). Phase composition and structure of aluminum Al–Cu–Si–Sn–Pb alloys. *Phys. Metals Metallogr.* 117, 579–587. doi: 10.1134/S0031918X16040025
- Belov, N. A., Stolyarova, O. O., and Yakovleva, A. O. (2016a). Effect of lead on the structure and phase composition of an Al–5% Si–4% Cu casting alloy. *Russ. Metall.* 2016, 198–206. doi: 10.1134/S0036029516030034
- Bravo, A. E., Durán, H. A., Jacobo, V. H., Ortiz, A., and Schouwenaars, R. (2013). Towards new formulations for journal bearing alloys. *Wear.* 302, 1528–1535. doi: 10.1016/j.wear.2013.01.040
- Bushe, N. A., Goryacheva, I. G., and Makhovskaya, Y. Y. (2003). Effect of aluminum-alloy composition on self-lubrication of frictional surfaces. *Wear.* 254, 1276–1280. doi: 10.1016/S0043-1648(03)00110-8
- Gershman, J. S., and Bushe, N. A. (2004). Thin films and self-organization during friction under the current collection conditions. *Surf. Coat. Technol.* 186, 405–411. doi: 10.1016/j.surfcoat.2003.11.016
- Mironov, A. E., Gershman, I. S., Gershman, E. I., and Zheleznov, M. M. (2017). Relationship between the tribological properties of experimental aluminum alloys and their chemical composition. *J. Frict. Wear.* 38, 87–91. doi: 10.3103/S1068366617020155
- Mironov, A. E., Gershman, I. S., Ovechkin, A. V., and Gershman, E. I. (2015). Comparison of scoring resistance of new antifriction aluminum alloys and traditional antifriction bronze. *J. Frict. Wear.* 36, 257–261. doi: 10.3103/S1068366615030095
- Panin, V. E., Grinyaev, Y. V., and Egorushkin, V. E. (2010). Foundations of physical mesomechanics of structurally inhomogeneous media. *Mech. Solids.* 45, 501–518. doi: 10.3103/S0025654410040023
- Rigney, D. A. (2000). Transfer, mixing and associated chemical and mechanical processes during the sliding of ductile materials. *Wear.* 245, 1–9. doi: 10.1016/S0043-1648(00)00460-9
- Sachek, B. Y., Mezrin, A. M., Muravyeva, T. I., and Stolyarova, O. O. (2016). The complex express evaluation of tribotechnical properties of antifriction aluminum alloys by sclerometric tests. *J. Frict. Wear.* 37, 469–475. doi: 10.3103/S1068366616050160
- Sachek, B. Y., Mezrin, A. M., Muravyeva, T. I., Stolyarova, O. O., Zagorskiy, D. L., and Belov, N. A. (2015). Investigation of the tribological properties of

- antifrictional aluminum alloys using sclerometry. *J. Frict. Wear.* 36, 103–111. doi: 10.3103/S1068366615020142
- Sachek, B. Y., Mezrin, A. M., Shcherbakova, O. O., Muravyeva, T. I., and Zagorskiy, D. L. (2018). Studies on the tribological properties and structure of antifrictional iron-containing aluminum alloys. *J. Frict. Wear.* 39, 206–214. doi: 10.3103/S1068366618030108
- Schouwenaars, R., Jacobo, V. H., and Ortiz, A. (2007). Microstructural aspects of wear in soft tribological alloys. *Wear.* 263, 727–735. doi: 10.1016/j.wear.2006.12.037
- Stolyarova, O. O., Muravyeva, T. I., Zagorskiy, D. L., and Gubenko, M. M. (2017). Investigation of the surface of antifriction Al–Cu–Si–Sn–Pb aluminum alloys. *J. Surf. Invest.* 11, 832–839. doi: 10.1134/S1027451017040292
- Zhang, S. C., Pan, Q. L., Jie, Y. A. N., and Huang, X. (2016). Effects of sliding velocity and normal load on tribological behavior of aged Al–Sn–Cu alloy. *Trans. Nonferrous Metals Soc. China.* 26, 1809–1819. doi: 10.1016/S1003-6326(16)64292-9
- Conflict of Interest Statement:** The authors declare that the research was conducted in the absence of any commercial or financial relationships that could be construed as a potential conflict of interest.
- Copyright © 2019 Mezrin, Shcherbakova, Muravyeva, Zagorskiy and Shkalei. This is an open-access article distributed under the terms of the Creative Commons Attribution License (CC BY). The use, distribution or reproduction in other forums is permitted, provided the original author(s) and the copyright owner(s) are credited and that the original publication in this journal is cited, in accordance with accepted academic practice. No use, distribution or reproduction is permitted which does not comply with these terms.